



Polyblend Nanofibers to Regenerate Gingival Tissue: A Preliminary *In Vitro* Study

Elena Canciani^{1*†}, Nicoletta Gagliano^{2†}, Francesca Paino¹, Evžen Amler^{3,4,5,6}, Radek Divin^{3,4,6}, Luca Denti², Dolaji Henin¹, Andrea Fiorati^{7,8} and Claudia Dellavia¹

¹Department of Biomedical, Surgical and Dental Sciences, Università degli Studi di Milano, Milan, Italy, ²Department of Biomedical Sciences for Health, Università degli Studi di Milano, Milan, Italy, ³Department of Tissue Engineering, Institute of Experimental Medicine of the Czech – Academy of Science, Prague 4, Czech Republic, ⁴Institute of Biophysics, 2nd Faculty of Medicine, Charles University, Prague 5, Czech Republic, ⁵Student Science s.r.o, Národních Hrdinů 279, Dolní Počernice, Prague, Czech Republic, ⁶UCEEB, Czech Technical University, Břestřevka, Prague, Czech Republic, ⁷Department of Chemistry, Materials and Chemical Engineering “G. Natta”, Politecnico di Milano, Milan, Italy, ⁸INSTM - Local Unit Politecnico di Milano, Milan, Italy

OPEN ACCESS

Edited by:

Fabricio Mezzomo Collares,
Federal University of Rio Grande do
Sul, Brazil

Reviewed by:

Gabriela Balbinot,
Universidade Federal do Rio Grande
do Sul, Brazil
Victor Pinheiro Feitosa,
Faculdade Paulo Picanço, Brazil

*Correspondence:

Elena Canciani
elena.canciani@unimi.it

[†]These authors have contributed
equally to this work and share first
authorship

Specialty section:

This article was submitted to
Biomaterials,
a section of the journal
Frontiers in Materials

Received: 19 February 2021

Accepted: 12 May 2021

Published: 04 June 2021

Citation:

Canciani E, Gagliano N, Paino F,
Amler E, Divin R, Denti L, Henin D,
Fiorati A and Dellavia C (2021)
Polyblend Nanofibers to Regenerate
Gingival Tissue: A Preliminary *In
Vitro* Study.
Front. Mater. 8:670010.
doi: 10.3389/fmats.2021.670010

Aim: The regeneration of small periodontal defects has been considered an important divide and challenging issue for dental practitioners. The aim of this preliminary *in vitro* study was to analyze the effects of polycaprolactone (PCL) nanofibers enriched with hyaluronic acid and vitamin E vs. nude nanofibers on gingival fibroblasts activity, an innovative graft for periodontal soft tissue regeneration purposes.

Methods: Nanofibers were produced in PCL (NF) or PCL enriched with hyaluronic acid and vitamin E (NFE) by electrospinning technique. NF and NFE were stereologically and morphologically characterized by scanning electron microscope (SEM), and composition was analyzed by infrared spectroscopy. Human fibroblasts were obtained from one gingival tissue fragment (HGF) and then seeded on NF, NFE, and plastic (CT). Cell adhesion and morphology were evaluated using SEM at 24 h and cell viability after 24, 48, and 72 h by alamarBlue[®] assay. Gene expression for COL-1, LH2b, TIMP-1, PAX, and VNC was analyzed by real-time RT-PCR in samples run in triplicate and GAPDH was used as housekeeping gene. Slot blot analysis was performed and immunoreactive bands were revealed for MMP-1 and COL-1. YAP and p-YAP were analyzed by Western blot and membranes were reprobated by α -tubulin. Statistical analysis was performed.

Results: IR spectrum revealed the presence of PCL in NF and PCL and vitamin E and hyaluronic acid in NFE. At 24 h, HGF adhered on NF and NFE conserving fibroblast like morphology. At 72 h from seeding, statistically significant differences were found in proliferation of HGF cultured on NF compared to NFE. Expression of genes (LH2b, TIMP-1, and MMP-1) and proteins (COL-1) related to collagen turnover revealed a reduction of COL-1 secretion in cells cultured on NF and NFE compared to CT; however, NFE stimulated cross-linked collagen deposition. Mechanosensor genes (PAX, VNC, and YAP) were upregulated in HGF on NF while they were decreased in cells grown on NFE.

Conclusion: Preliminary data suggest that PCL-enriched nanofibers could represent a support to induce HGF proliferation, adhesion, collagen cross-linking, and to reduce collagen degradation, therefore favoring collagen deposition in gingival connective tissue.

Keywords: polycaprolactone, hyaluronic acid, vitamin E, nanofibers, oral soft tissues regeneration, gingival fibroblasts, collagen turnover

INTRODUCTION

Patients' aesthetic expectation and awareness about oral health have considerably increased in last years. The regeneration of small periodontal defects has been considered an important and challenging issue for dental practitioners (Hatayama et al., 2017; Rasperini et al., 2020). Periodontal plastic surgery is the gold standard for correcting the morphology of gingival defects. However, surgical interventions have shown to be unpredictable for long-term stability of the sites (Hägi et al., 2014).

Recently, numerous technologies and materials have been developed in order to promote periodontal soft tissue regeneration by means of three-dimensional (3D) supports that stimulate the biological process of the connective tissues (Botelho et al., 2017).

An ideal scaffold for connective tissue engineering, to stimulate cellular biological processes, should have several features: support cell growth by 3D topography mimicking extracellular matrix (ECM), have a high surface-to-volume ratio, have the presence of many interconnected pores for blood vessels passage, and have the possibility to be functionalized or to be composed by several materials.

Synthetic polymers, such as polycaprolactone (PCL), are largely used in several fields of regenerative medicine, including dentistry, to create bio-printed scaffolds for periodontal osseous defect treatment (Rasperini et al., 2015) and to produce nanofibers to stimulate human dental pulp-derived stem cells activity (Mohandesnezhad et al., 2020). Furthermore, PCL allows to produce miscible polyblend with natural polymers (Gunn et al., 2010) and substances.

Polyblend nanofibers represent an innovative biomimetic synthesized material in nanoscale with great potential to create 3D scaffolds for their physical, chemical, and morphological features. During the healing process and tissue regeneration, nanofibers provide mechanical support and structural guidance for cellular growth, exploiting properties of the native tissue and releasing chemical cues (Gunn et al., 2010; Amler et al., 2014). Thus, numerous are the advantages to design polyblend nanofibers. On one side, polyblending would allow to control physicochemical features such as morphology, wettability, formulation, mechanical strength, (Carter et al., 2016); on the other side, polyblending would allow to stimulate biological activity of cells, favoring cell attachment, proliferation, and differentiation (Beznoska et al., 2019).

In the literature, miscible polyblend PCL based have been recently tested to improve wound healing (Amler et al., 2014). Chanda et al., (2018) studied an electrospun scaffold consisting of chitosan, PCL, and hyaluronic acid (HA) to enhance proliferation, growth, and migration of Vero cell.

Further with the presence of HA, it aimed to mechanically stabilize the scaffold (Chanda et al., 2018). Kalantary et al., (2020) charged PCL/gelatin nanofibers with vitamin E to produce a device able to protect skin from ROS (reactive oxygen species) released after occupational skin exposure (Kalantary et al., 2020). The authors demonstrated that nanofibers containing vitamin E showed a higher viability compared to PCL/gelatin ones and significantly assisted human skin cells against *tert*-Butyl hydroperoxide (t-BHP)-induced oxidative stress (Kalantary et al., 2020). Although PCL nanofibers were previously studied, the behavior of gingival fibroblasts in contact with PCL nanofibers enriched with vitamins for tissue regeneration and wound healing has not yet been largely investigated.

Hyaluronic acid is a natural glycosaminoglycan, an essential molecule of the connective tissue of the oral mucosa and the skin, which plays a pivotal role in numerous processes such as wound healing (Alexander et al., 1980). HA is a well-known natural hydrogel. In fact, it is able to maintain ECM resilience and tissue hydration, to create temporary structure for deposition of ECM proteins, to trigger cell adhesion, proliferation, and migration. It was demonstrated that HA regulates vascular endothelial cell function (Mesa et al., 2002; Tammi et al., 2002; Litwiniuk et al., 2016; Canciani et al., 2021) giving beneficial effect when used in the treatment of diabetic wound ulcers (Chen et al., 1999; Voigt et al., 2012). HA is biocompatible, biodegradable, bacteriostatic, antioxidant, anti-edematous, and finally anti-inflammatory (Fraser et al., 1997; Pirnazar et al., 1999; Campo et al., 2012). HA is used in various fields of medicine and also in dentistry (Robert et al., 2015; Eliezer et al., 2019); a systematic review and meta-analyses reported that seems to favor periodontal healing after surgical procedures (Bertl et al., 2015).

Vitamin E is known to have a key role in the prevention of many pathogens thanks to its anti-inflammatory effects (Konieczka et al., 2019). It is therefore a pivotal nutrient in dermatological application (Thiele et al., 2005) because it seems to affect collagen turnover to improve wound healing (Hobson, 2016).

The aim of this preliminary *in vitro* study was to analyze the effects of PCL nanofibers enriched with HA and vitamin E (NFE) vs PCL nanofibers alone (NF) on the gingival fibroblast activity assessing morphology, viability, collagen turnover, and mechanosensing.

MATERIALS AND METHODS

Nanofibers Production and Characterization

Nanofibers tested in the experiment were produced in PCL or PCL enriched with HA and vitamin E.

NF was obtained from a solution of 14% (w/v) of PCL, with a molecular weight (MW PCL) of 45,000 Dalton (Sigma-Aldrich, MO, United States) dissolved in chloroform:ethanol (8:2) (Plencner et al., 2014). NFE were obtained as described above but adding to the solution of hyaluronic acid (HA) at 0.002% (Sigma-Aldrich, MO, United States) and vitamin E at 0.0014% (α -Tocopherol; Sigma, St. Louis, MO). The concentration of the enriching agents (HA and vitamin E) was chosen in accordance with our previous work (Canciani et al., 2021), also taking into account that higher concentrations of HA and vitamin E could cause structural defects in 3D nanofiber's structure. This emulsion was prepared and preserved from light due to the photosensitivity of the vitamin. Electrospinning was performed using a Nanospider TM device (Elmarco, Czech Republic) (Amler et al., 2014). A high-voltage source generated voltage of up to 56 kV, and the polymer solutions were connected to the high-voltage electrode. The electrospun nanofibers were deposited on a grounded collector electrode. The distance between the tip of the syringe needle and the collecting plate was 12 cm. For both NF and NFE, one sheet of 50 × 50 cm was produced. All electrospinning processes were performed at room temperature (RT; ~24°C) and a relative humidity of ~50%.

Characterization of NF and NFE samples was performed by means of attenuated total reflection Fourier transform infrared spectroscopy (ATR-FTIR). The ATR-FTIR spectra were recorded at T = 298 K, under nitrogen atmosphere, in a 550–4,000 cm⁻¹ wavelength range using an Agilent Cary 640-IR infrared spectrometer (Agilent Technologies, Santa Clara, CA, United States) equipped with a single bounce ZnSe ATR accessory. All the spectra were collected in triplicate.

Mechanical properties of five 0.5 × 2 cm² pieces obtained from the produced sheets were preconditioned in PBS for 10 min, and these wet pieces were evaluated by a dynamic mechanical analyzer (DMA) (TA, Q800). The DMA strain rate was 0.02 min⁻¹; tensile test was performed with a preload of 1 mN at room temperature.

Biodegradability test was performed by a stereomicroscope (SZX Olympus instruments), leaving nanofibers for 28 days in a phosphate buffer saline (PBS) solution.

Morphological analysis was effectuated by scanning electron microscope (SEM) (Tescan Vega 3, Brno, Czech Republic) to verify the nanofiber's diameter and largest pore size by means of image analysis software (Vega3 SB, Tescan a.s). For both NF and NFE, three random 0.8 × 0.8 cm² pieces of the produced sheets were selected and three 80 × 80 μm² areas were analyzed on each piece. For each area, 5 measurements of largest pores and nanofiber's diameter were executed. Nanofiber's diameter distribution was obtained and the largest pore range was computed.

Cell Cultures of Primary Gingival Fibroblasts (HGF)

During molar extraction appointment, following local anesthesia, using articaine with epinephrine 1:100,000 (Pierrel Pharma S.P.A., Zurich), a surgical incision was performed to expose

the impacted tooth in a female patient, 35 years old, and after the extraction, the flaps were sutured (Vycril 3/0). The patient was free from periodontal diseases, did not use hormonal contraceptives or hormonal replacement medications, and signed a consent form to participate in the experiment. The study was conducted in accordance with the ethical principles of the World Medical Association Declaration of Helsinki and the local Ethics Committee of Università degli Studi di Milano, Milan (29/18 of the 28 June 2018). Exceeded soft tissue biopsy was collected to obtain HGF.

Bioptical fragment was washed with sterile PBS and incubated in a solution of DMEM (Dulbecco's Modified Eagle Medium) and collagenase I 4 mg/ml (Millipore, United States). Cell suspension was filtered and plated in a T25 flask. Cells were cultured at 37°C in a 5% CO₂ humidified incubator in a DMEM containing 10% heat-inactivated fetal bovine serum (FBS) (GIBCO), supplemented by 100 U/mL penicillin (Invitrogen), 100 μg/mL streptomycin (GIBCO), 2.5 μg/mL amphoterycin B (Sigma), and adding ascorbic acid (200 μM) (Francetti et al., 2019).

For the analysis, cells were seeded on a plastic or on nanofibers in 6- or 24-well multi-well plates at the concentration of 1.5 × 10⁴. HGF were used between the fourth and the fifth passage, approximately at 80% confluence, and molecular evaluations were performed in samples cultured for 72 h on NF, NFE, or on plastic (CT). Primary HGF were tested for viability and adhesion. Furthermore, genes and proteins expression related to collagen turnover and mechanotransduction pathways were also evaluated. Two replicate experiments for both NF and NFE were performed. In each experiment, a technical triplicate was applied and conducted at 37°C in a 5% CO₂ humidified incubator.

Viability Test by alamarBlue

To test cell viability, 7 × 10³ cells were seeded on NF and NFE in 24-well multi-well plates. Cell viability was tested at 3 different time points (24, 48, and 72 h from seeding) using alamarBlue® (Thermo Fisher Scientific), a test that allows to determine a proliferation curve related to the metabolic cellular ability.

The color changing of the culture medium reveals an active cellular metabolism, and it was monitored and read by a spectrophotometer (Glo Max Discover, Promega Corporation, United States). For each group, a proliferation curve was created, and the % of cells proliferation was calculated in relation to CT proliferation, inserting the values in an algorithm, as described by the manufacturer's protocol.

Cell Adhesion and Morphology

Cell adhesion and morphological assessment of spreading of the cells on NF and NFE were evaluated after 24 h from seeding. Morphological analysis was performed on images acquired using SEM. In brief, the samples were fixed with 2.5% glutaraldehyde, postfixed in osmium tetroxide, dehydrated through an increasing scale of alcohol, infiltrated with hexamethyldisilane, and dried. Finally, the samples were mounted on stubs and coated with a thin layer of gold. The fields to analyze were acquired at a total

magnification until 1,000x by means of a Jeol Neoscope Electron Microscope (JCM-6000; Nikon, Tokyo, Japan). Cell morphology was analyzed, with particular attention to observe the presence of cytoplasmic extensions, functional orientation, and cell arrangement on the surface (Canciani et al., 2016).

Real-Time PCR

Cells were harvested and the total RNA was isolated (Tri Reagent, Sigma, Italy). One μg of total RNA was reverse transcribed in a 20 μL final volume of reaction mix (Bio-Rad, Segrate, Milan, Italy). mRNA levels for long type I collagen (COL-I), lysyl hydroxylase 2 (LH2b), and tissue inhibitor of matrix metalloproteinase 1 (TIMP-1) were analyzed by real-time RT-PCR in samples run in triplicate. Glyceraldehyde 3-phosphate dehydrogenase (GAPDH) was used as housekeeping gene to normalize the differences in the amount of total RNA in each sample. The primers sequences were the following: GAPDH: sense CCCTTCATTGACCTCAACTACATG, antisense TGG GATTTCCATTGATGACAAGC; LH2b: sense CCGGAAACA TTCCAAATGCTCAG, antisense GCCAGAGGTCATTGTTAT AATGGG; TIMP-1: sense GGCTTCTGGCCTCCTGTTGTTG, antisense AAGGTGGTCTGGTTGACTTCTGG; PAX sense CAGCAGACACGCATCTCG, antisense GAGCTGCTCCCT GTCTTCC; VNC sense GGAGGTGATTAACCAGCCAAT, antisense AATGATGTCATTGCCCTTGC. Each sample was analyzed in triplicate in a Bioer LineGene 9600 thermal cycler (Bioer, Hangzhou, China). The cycle threshold (Ct) was determined and gene expression levels relative to that of GAPDH were calculated using the ΔC_T method.

Slot Blot

Slot blot analysis was performed in serum-free cell culture supernatants. Cell culture media protein content was determined by a standardized colorimetric assay (DC Protein Assay, Bio-Rad, Italy); 100 μg of total protein per sample in a final volume of 200 μL of Tris buffer saline (TBS) was spotted onto a nitrocellulose membrane in a Bio-Dot SF apparatus (Bio-Rad, Italy). Membranes were blocked for 1 h with 5% skimmed milk in TBST (TBS containing 0.05% Tween-20), pH 8, and incubated for 1 h at room temperature in a monoclonal antibody to COL-I (1:1,000 in TBST) (Sigma-Aldrich, Milan, Italy) and MMP-1 (1 $\mu\text{g}/\text{ml}$ in TBST, Millipore, Milan, Italy). After washing, membranes were incubated in HRP-conjugated rabbit anti-mouse serum (1:6,000 in TBST to detect COL-I; 1:20,000 in TBST to detect MMP-1) (Sigma, Italy) for 1 h. Immunoreactive bands were revealed by the Opti-4CN substrate or Amplified Opti-4CN substrate (Bio-Rad, Italy) and scanned densitometrically (UVBand, Eppendorf, Italy).

Western Blot

Whole cell lysates were prepared in a lysis buffer (Tris-HCl 50 mM pH 7.6, 150 mM NaCl, 1% Triton X-100, 5 mM EDTA, and 1% sodium dodecyl sulphate), proteases inhibitors, and 1 mM sodium orthovanadate. Lysates were incubated in ice for 30 min and centrifuged at 14,000 $\times g$ for 10 min at 4°C. Cell lysates (30 μg of total proteins) were run on 10% SDS-polyacrylamide gel, separated under reducing and

denaturing conditions at 80 V according to Laemmli, and transferred at 90 V for 90 min to a nitrocellulose membrane in 0.025 M Tris, 192 mM glycine, and 20% methanol, pH 8.3. Membranes were incubated with YAP (1:1,000 dilution, D8H1X, Rabbit mAb, Cell Signaling) or p-YAP (S109) (1:1,000 dilution, D3I6D Rabbit mAb, Cell Signaling). After the incubation with a horseradish peroxidase (HRP)-conjugated goat anti-rabbit antibody (1:20,000 dilution, Cell Signaling), immunoreactive bands were revealed using the Amplified Opti-4CN (Bio-Rad).

Membranes were reprobated by monoclonal antibody to α -tubulin (1:2,000 dilution, Sigma-Aldrich) to confirm equal loading.

Statistical Analysis

Descriptive analysis was performed and mean and standard deviation (SD) of the values obtained from the two experimental technical triplicates were computed for both NF and NFE samples in all performed tests. A nonparametric statistical analysis by Wilcoxon rank-sum test was used to compare the results of the mechanical characterization of NF and NFE, and a p value < 0.05 was considered significant (GraphPad Software Inc., San Diego).

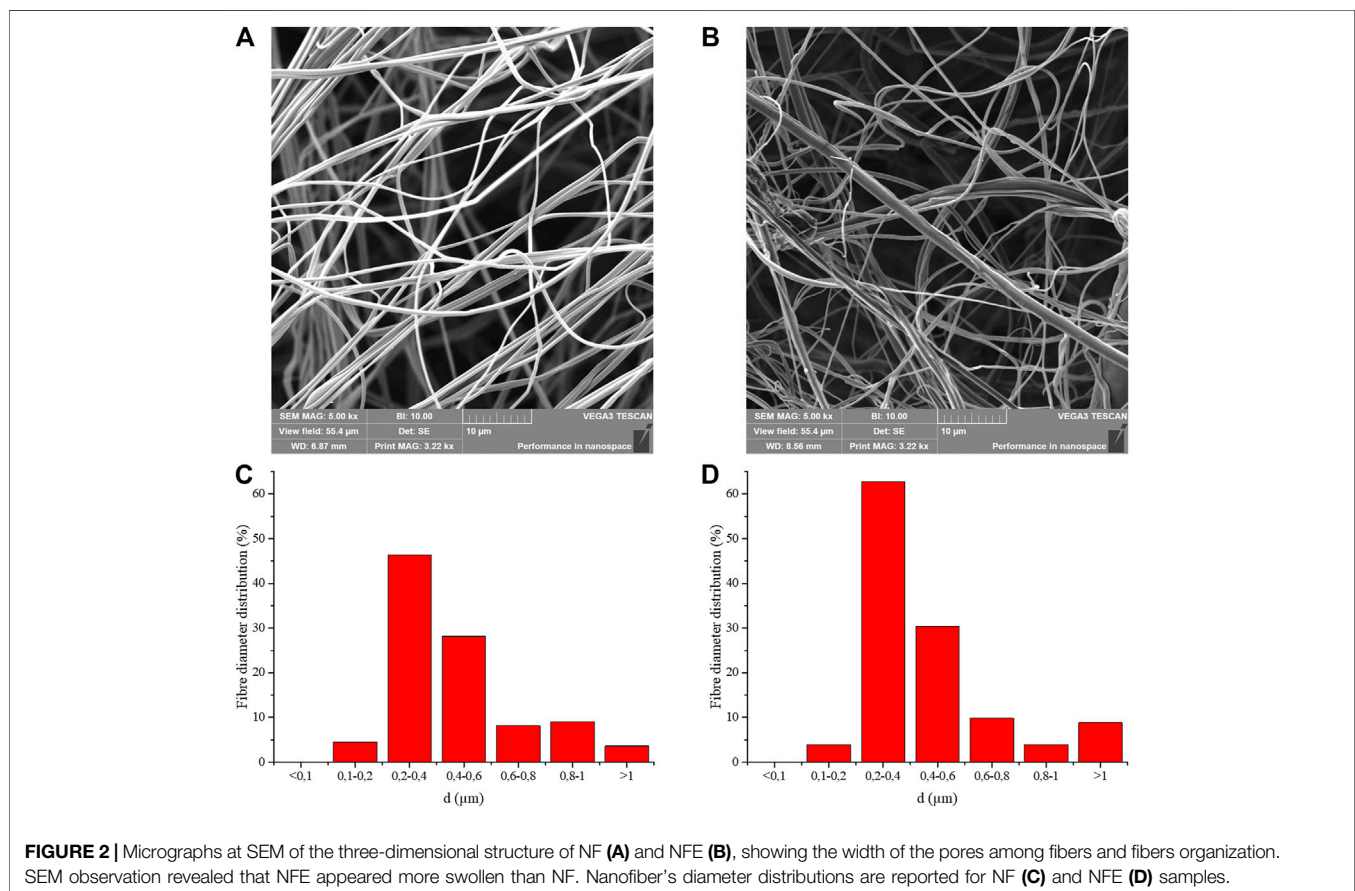
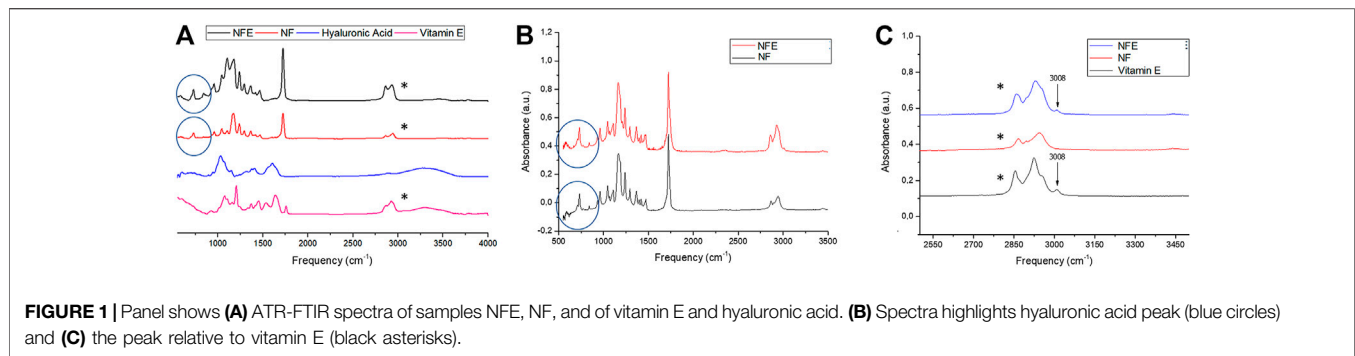
Comparisons between NF and NFE mean values were performed at each time point of the viability test by means of paired t -test with a level of significance of $p < 0.05$ (GraphPad Software Inc., San Diego, CA 92108, United States). Differences associated with p values lower than 5% were to be considered statistically significant.

RESULTS

Nanofibers Characterization

In **Figure 1** are reported the ATR-FTIR spectra of the specimens (NFE and NF) and of the corresponding enriching agents (HA and vitamin E). As expected, the spectra of the unloaded nanofibers samples (NF) show only signals which can be attributed to the PCL used as starting materials (Primpke et al., 2018). The enriched specimens (NFE) possess ATR-FTIR spectra which are composed mainly of the signals of PCL; however, the presence of a broadened peak at about 3,400 cm^{-1} , typical of O-H stretching vibrations, the broadening of the signal at 1,176 cm^{-1} , and the growth of the peak at 1,103 cm^{-1} suggest the proper loading of HA and vitamin E in the samples NFE. (**Figure 1A**). HA presence influences the spectrum from 500 to 700 cm^{-1} by increasing the values in NFE compared with NF as illustrated in figure B (**Figure 1B**). Furthermore, considering vitamin E, a peak around 3,008 cm^{-1} was observed, thus confirming its incorporation in NFE sample (**Figure 1C**). NF showed a higher but not statistically significant stress at break than NFE (1.47 ± 0.34 MPa vs 1.06 ± 0.25 MPa, $p > 0.05$). In contrast, deformation at break was significantly higher in NF than in NFE ($31.52 \pm 5.08\%$ vs $14.11 \pm 4.64\%$, $p < 0.01$). Strain resulted statistically significant between NF and NFE for p value < 0.01 .

Biodegradability observation showed that after 28 days the nanofibers had maintained their structure.



NF and NFE morphology was assessed by SEM (Figures 2A,B) showing the typical organization of nanofibers in a mesh characterized by fibers of different dimension size and interconnection. Fiber's diameters presented a Gaussian-like distribution with a prevalent percentage of fibers in the range between 0.2 and 0.4 μm for both groups (Figures 2C,D). In NFE, the encapsulation of HA and vitamin E determined a shift of the distribution toward larger diameters (Figure 2D).

Due to difficulty in measuring the space of an irregular mesh on a bidimensional SEM image, the distance between the farthest nanofibers was calculated in the largest pores. In NF, the largest

distance calculated was $86.98 \pm 25.60 \mu\text{m}$ (Figure 2A), while in NFE, it was $31.66 \pm 7.97 \mu\text{m}$ (Figure 2B).

Fibroblasts Morphology and Adhesion on NF and NFE

After seeding, HGF grew in adhesion on nanofibers. HGF morphological features were evaluated by SEM (Figure 3). One day after seeding, fibroblasts were housed on the surface of NF (Figure 3A) and NFE (Figure 3B).

HGF showed cytoplasmic protrusions extending on nanofibers used as rails (Figure 3A) and becoming in contact.

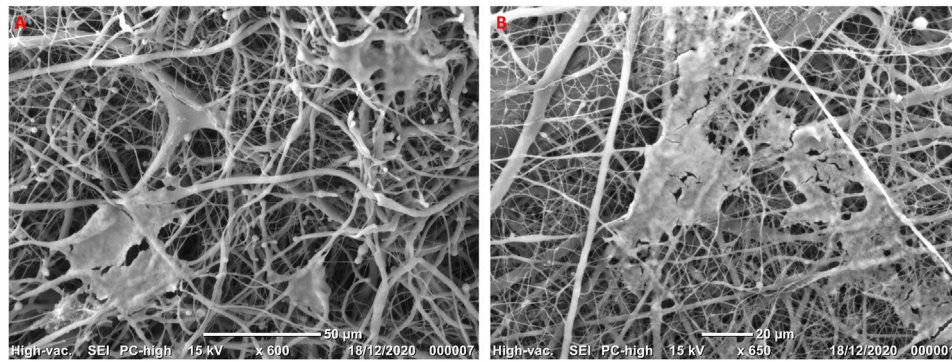


FIGURE 3 | Representative micrographs at SEM showing HGF cultured on NF (A) and NFE (B) highlighting the three-dimensional structure of nanofibers and cells that seem to be interconnected.

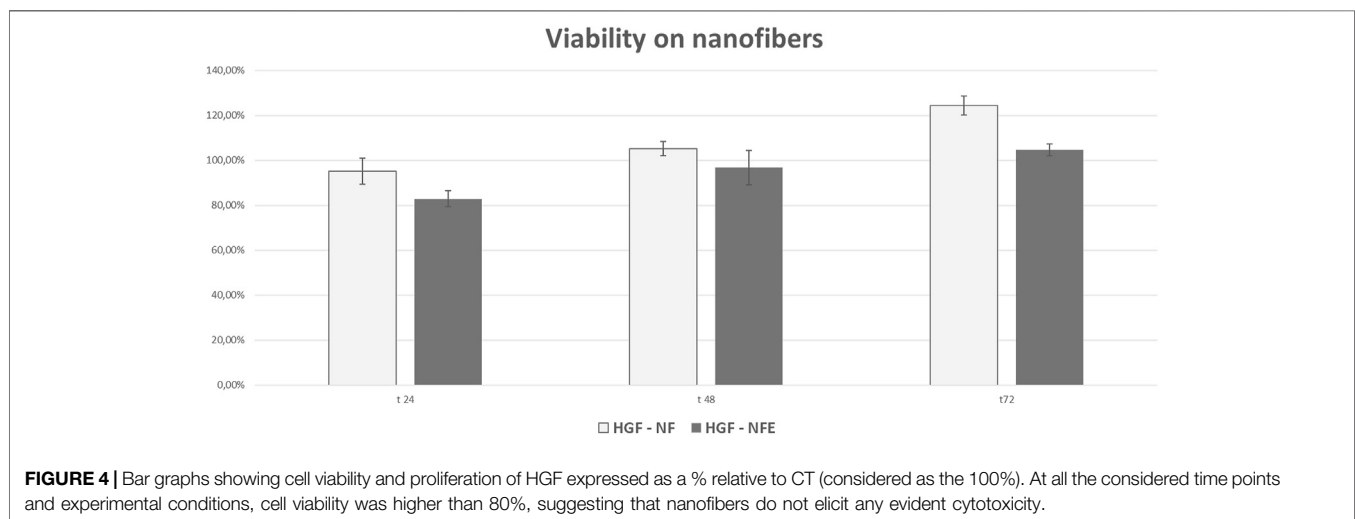


FIGURE 4 | Bar graphs showing cell viability and proliferation of HGF expressed as a % relative to CT (considered as the 100%). At all the considered time points and experimental conditions, cell viability was higher than 80%, suggesting that nanofibers do not elicit any evident cytotoxicity.

Moreover, they were arranged rolling up or reclining on nanofibers, in particular on NF samples. On the other hand, when cells grew on NFE, they extended across the pores creating bridges to build a network to cover the nanofibers mesh surface (Figure 3B).

Viability of HGF on NF and NFE

AlamarBlue® test evaluation at early time points revealed that the metabolism of HGF was not affected by NF and NFE. A trend of viability reduction was observed at 24 and 48 h after seeding in all experimental groups, considering 100% the viability reference of the CT. At 72 h from seeding, HGF cultured both on NF and NFE showed values over control threshold (Figure 4).

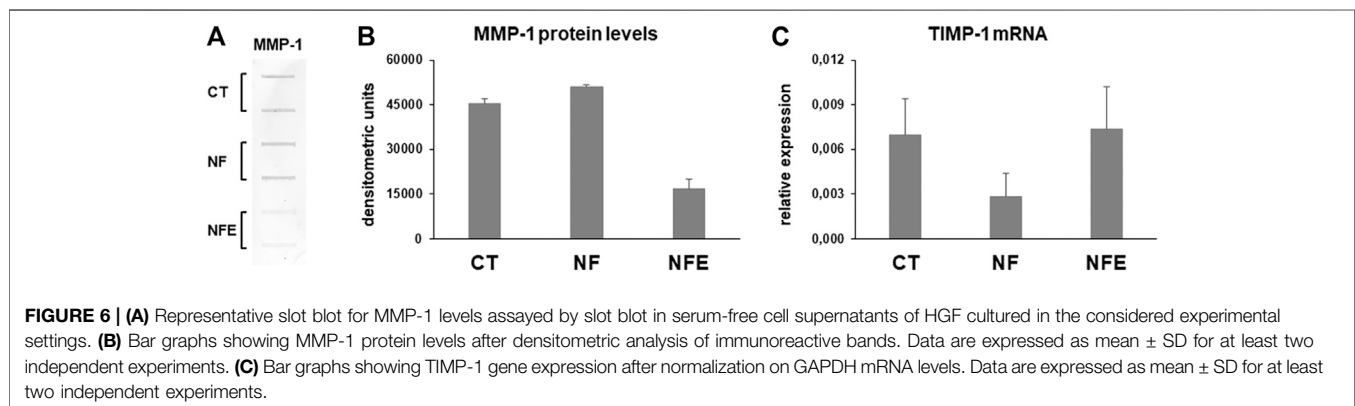
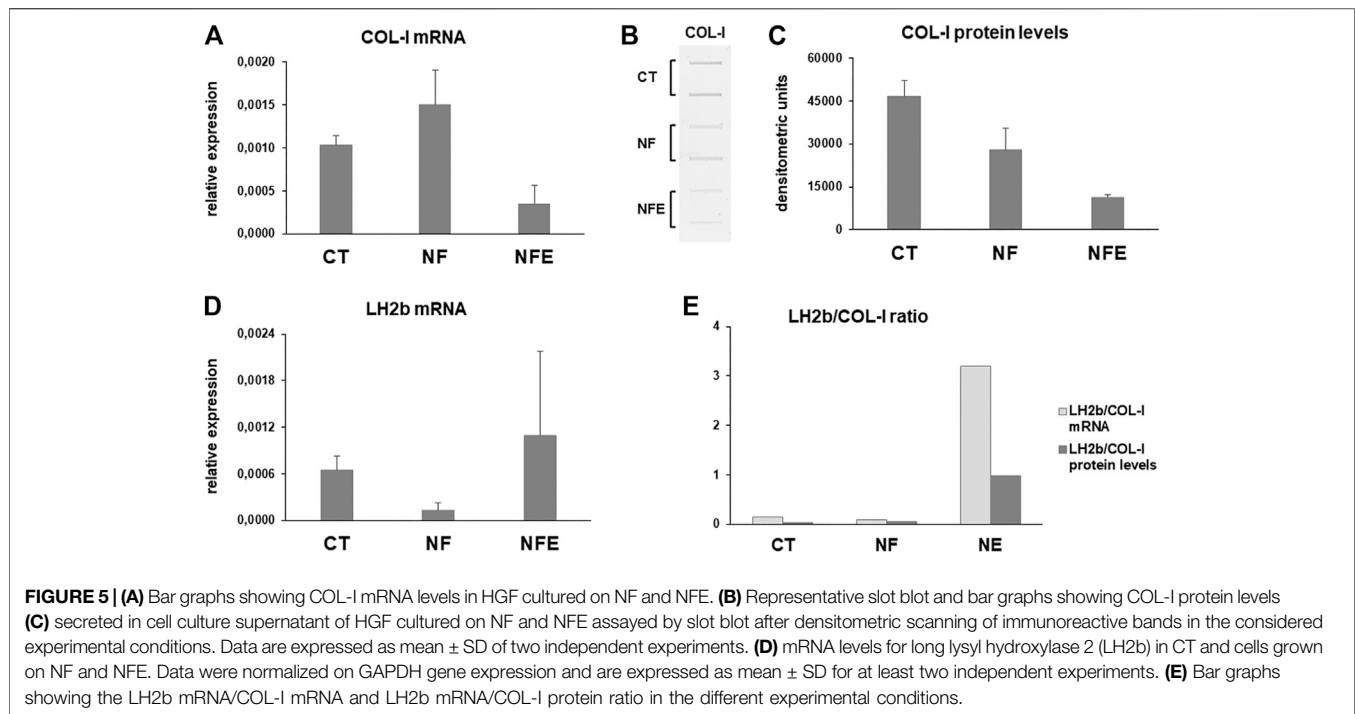
Expression of Genes and Proteins Related to Collagen Turnover

Type I collagen (COL-I) mRNA levels were increased in cells grown on nanofibers (+45% vs CT), while a strong downregulation was evident in fibroblasts cultured on NFE

(−66%) (Figure 5A). COL-I protein levels secreted by HGF in cell culture supernatants were assessed by slot blot. COL-I protein levels revealed that the secretion of COL-I was reduced in cells cultured on NF (−39% vs CT) and on NFE (−75%) (Figures 5B,C).

Newly synthesized collagen undergoes maturation by covalent cross-linking after hydroxylation of amino acids such as lysine. Collagen maturation was assessed by analyzing the mRNA levels for LH2b by real-time PCR. LH2b mRNA levels showed a different pattern of expression in all experimental conditions. In fact, LH2b resulted downregulated and upregulated, respectively, in HGF cultured on NF and NFE, compared to CT (Figure 5D). The LH2b mRNA/COL-I mRNA and LH2b mRNA/COL-I protein ratio shows a strong increase in cells grown on NFE (Figure 5E), pointing to an increased collagen cross-linking in this experimental condition.

Interstitial collagen degradation was assessed by slot blot analysis of MMP-1 levels in cell culture supernatants. Our data show that MMP-1 levels were similar in supernatants of



HGF on NF and CT but were downregulated when cells are grown on NFE (**Figures 6A,B**). Gene expression analysis for TIMP-1 mRNA revealed that its expression was decreased in cells grown on NF but was unchanged in cells cultured on NFE (**Figure 6C**).

Expression of PAX, VNC, and YAP as Mechanosensors

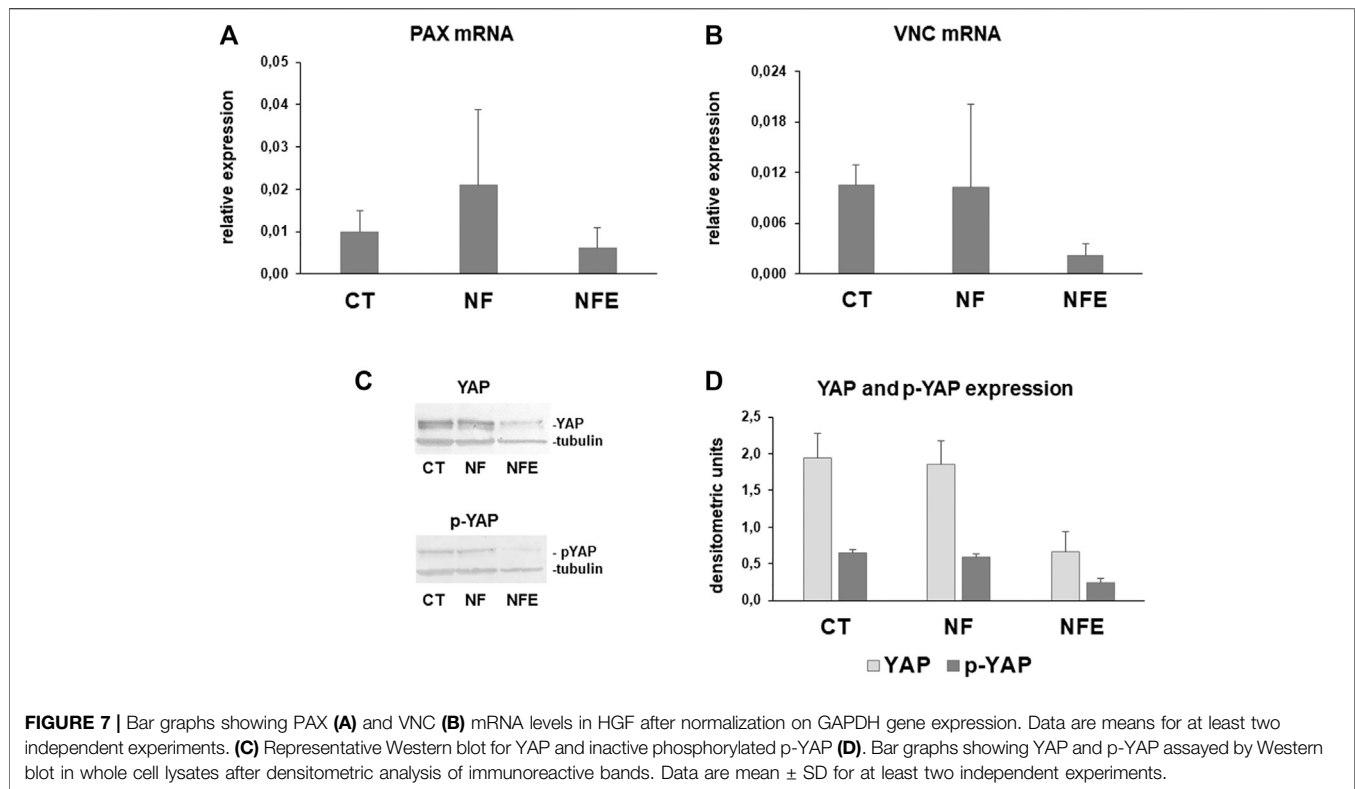
To better understand whether NF exert any mechanical effect on collagen turnover pathways, we analyzed the expression of mechanosensors such as PAX, VCN, and YAP. PAX and VCN are components of the adhesion plaque and also act as mechanosensors. Their mRNA levels were tended to be upregulated in HGF on NF, while they were decreased in cells grown on NFE (**Figures 7A,B**).

Yes-associated protein (YAP) is a mechanosensor that can be inactivated by phosphorylation, leading to cytoplasmic translocation. YAP and p-YAP were analyzed by Western blot. YAP and p-YAP resulted similarly expressed in cell lysates obtained from CT and HGF on NF. By contrast, a strong downregulation was evident in fibroblasts grown on NFE (**Figures 7C–G**).

DISCUSSION

To date, dental practitioners still have to face a challenging issue to restore a proper morphology of the oral soft tissue due to periodontal disease.

The development of new technologies and devices may help in the regeneration of the oral soft tissues, thus allowing to obtain a physiologically stable masticatory apparatus and to reach an



optimal aesthetic. An emerging and increasingly widespread innovation in dentistry is the use of nanotechnologies for oral tissue regeneration (Ahadian et al., 2020; Bonilla-Represa et al., 2020; Mohandesnezhad et al., 2020).

In the current preliminary study, the authors were interested in evaluating the biological activity of primary HGF fibroblasts obtained from one patient on polyblend nanofibers exhibiting two key characteristics: they have a texture similar to the native ECM (Seo-Jin et al., 2016) and they can be loaded with compounds that stimulate resident cells (Bhattarai et al., 2018).

Several studies proposed the use of nanofibers to regenerate (Gunn et al., 2010; Chanda et al., 2018) or deliver substances and compounds (Amler et al., 2014; Ahadian et al., 2020) in different tissues (Wang et al., 2017; Beznoska et al., 2019); however, only few preliminary published articles are available in oral fields (Bonilla-Represa et al., 2020; Mohandesnezhad et al., 2020).

Due to their biological properties, in this study, we charged nanofibers with HA and vitamin E in order to characterize their impact on HGF metabolism and the possible effect on ECM deposition turnover.

The concentration of HA and vitamin E used in this study allowed to obtain nanofibers with a stable fibrillar structure organized in an irregular mesh, similar to the architecture of the extracellular matrix. The addition of these molecules determined the increase of the fiber's diameter with a consequent reduction of the pore dimensions, and a trend of reduction about mechanical properties was observed. In particular, NFE presented a significant reduction of the strain value compared to NF.

Due to these characteristics, polyblend nanofibers are supposed to be able to guide cells during their adhesion and proliferation, to bind water and therefore increase the volume *in situ*, and to act as a reserve of substances able to influence the quality of the ECM in accordance with the literature (Gunn et al., 2010).

All these features could be exploited to improve aesthetics and function in clinical procedures such as ridge augmentation (Dellavia et al., 2014).

In order to understand whether polyblend PCL nanofibers are a suitable device for HGF, this *in vitro* preliminary study analyzed HGF phenotype. For this purpose, in line with future clinical application, proliferation, adhesion, and collagen turnover pathways were evaluated. In fact, collagen is the main component of the gingival dense irregular connective tissue. Our results show that HGF were able to proliferate and adhere when cultured on both NF and NFE. However, SEM analysis revealed a different behavior of HGF between the two experimental groups. In fact, NF seemed to favor cell motility toward fibers, while cells grown on NFE seemed to be in closer contact and to form interconnecting bridges. These preliminary results suggested that NF and NFE likely affect cell adhesion and migration at a different extent and further experiments will be performed to analyze this effect.

We focused on collagen turnover pathways since COL-I is the main component of gingival connective tissue ECM. Its content is finely regulated by a balanced turnover controlled by HGF at the level of collagen synthesis, maturation, and degradation. Collagen turnover, therefore, is pivotal in influencing gingival connective tissue homeostasis. Our results show a nonsynchronous regulation of COL-I at the gene and protein expression in

fibroblasts cultured on NF, likely due to translational or posttranslational regulation mechanisms. By contrast, both COL-I mRNA and protein levels were decreased in cells grown on NFE compared to CT and NF. This finding suggests a reduced COL-I secretion induced by NFE. However, to predict the ability of fibroblasts to increase COL-I deposition in the gingival connective tissue, collagen maturation played by LH2b should also be considered. In fact, posttranslational hydroxylation of collagen by LH is a key mechanism of collagen maturation and ECM stability and, therefore, strongly influences collagen content. We analyzed LH2b gene expression since this is the major form expressed in all tissues. Moreover, LH2b is generally over-expressed in fibrotic processes and is responsible for the over-hydroxylation of the COL telopeptides, forming COL pyridinoline cross-links and, thus, contributing to unwanted COL accumulation. The LH2b mRNA/COL-I mRNA ratio indicates the gene expression of LH2b relative to COL-I and, therefore, is considered as an indicator of the susceptibility of collagen to undergo hydroxylation (Silver et al., 2000; Walker et al., 2005). Our results show that LH2b is downregulated by NF, while a very evident increase is induced in cells cultured on NFE. This finding suggests that NFE seem able to stimulate COL-I maturation by cross-linking to improve its stability and, therefore, favoring its deposition.

Collagen content is determined by the finely regulated dynamic balance between its synthesis and degradation by MMPs. Interstitial collagen breakdown is played by MMP-1, that cleaves the native triple helix of interstitial collagens into characteristic 3/4- and 1/4-collagen degradation fragments, also known as gelatins (Sakai et al., 1967), that can be further degraded to complete digestion by less specific proteinases such as MMP-2 (Sakai et al., 1967; Woessner et al., 1991).

MMP-1 is regulated at the posttranslational level by TIMP-1, the main inhibitor of MMP-1, that binds MMP-1 in a 1:1 stoichiometric ratio and inhibits its activation and activity (Murphy et al., 1994; Brew et al., 2001). Our results show that MMP-1 is similarly expressed in cell culture supernatants from CT and cells cultured on NF but it was strongly downregulated by NFE. This finding leads to the hypothesis that NFE are likely able to decrease COL-I degradation, and moreover, due to a higher cross-linking, they could favor COL-I accumulation in gingival connective tissue. This hypothesis is strengthened by the analysis of TIMP-1 mRNA levels that are highly expressed in HGF cultured on NF, therefore suggesting a further inhibition of COL-I degradation by NFE. These preliminary results suggest that HA in NFE could exert a role in influencing collagen degradation and are consistent with previously reported data showing that in HA cultures of fibroblasts a different collagen turnover pattern was observed when compared to collagen or collagen–fibrin cultures, mainly associated to a decrease in collagen synthesis (Chopin-Doroteo et al., 2018).

Mechanotransduction is the ability of cells to translate mechanical stimuli into biochemical signals that can influence gene expression, cell morphology, and cell fate. Mechanotransduction allows cells to respond to external forces and timely adapt their activity in ECM by remodeling (Jansen et al., 2015). To better understand whether nanofibers could exert any mechanical effect on HGF collagen turnover pathways, we

analyzed the expression of mechanosensors such as PAX, VCN, and YAP in HGF cultured on NF and NFE. In particular, YAP acts as a mechanosensor whose activity is primarily regulated by the substrate on which cells adhere by phosphorylation, leading to protein inactivation and cytoplasmic translocation (Dupont et al., 2005; Totaro et al., 2018). Our preliminary data suggest a different effect induced by NF and NFE on collagen turnover pathways in HGF. Since ECM remodeling and homeostasis in connective tissues are influenced also by mechanical stimuli and fibroblasts are mechanoresponsive cells, we were interested in understanding if HGF cultured on NF or NFE are differently influenced in sensing mechanical signals and convert them into biological responses (Burrige et al., 2016; Wang et al., 2012). For this purpose, we analyzed the expression of key mechanosensors. mRNA levels for PAX and VNC resulted in expressed at a lower extent in cells cultured on NFE, suggesting that HA could be able to reduce the mechanoresponsive response of HGF. This hypothesis is consistent with YAP and p-YAP pattern. In fact, they resulted similarly expressed in CT and in cells cultured on NF, while a strong downregulation was induced by NFE. These preliminary findings seem to suggest that NF nanofibers do not affect the response to mechanical response of HGF, while the presence of HA used to charge the NFE nanofibers downregulated PAX and VNC mRNA levels as well as YAP and p-YAP expression. To explain this effect, we can hypothesize that HA interaction with its CD44 receptor could likely modulate fibroblast adhesion to the substrate, thus influencing fibroblast behavior (Price et al., 2005).

Considered as a whole, these preliminary data show that NF and NFE elicit a different effect on HGF. NF seem to favor COL-I degradation by reducing TIMP-1 mRNA levels and, therefore, MMP-1 inhibition. Moreover, LH2b mRNA levels are also downregulated, pointing to a less cross-linked collagen. Since a not evident mechanical response is triggered by NF on fibroblasts, we can hypothesize that these effects induced by NF on HGF are not primarily based on a mechanical response. Conversely, NFE seem to exert an opposite effect compared to NF. In fact, they favor collagen cross-linking and inhibit collagen degradation, thus favoring its deposition. This effect seems to be related to a reduced mechanical stimulation exerted by HA on HGF. However, the current preliminary results were obtained in only one sample, thus needing further experiments to confirm our hypothesis and to understand if the effect of HA used to charge the NFE involves other alternative mechanisms different from the mechanotransduction.

CONCLUSION

Considered as a whole, these preliminary *in vitro* findings suggest that PCL-enriched nanofibers (NFE) could represent a device to enhance HGF proliferation and biosynthetic phenotype, likely favoring collagen deposition in the gingival connective tissue. However, further experiments are needed to confirm these results and the mechanism responsible of NFE biological activity on a higher number of samples, in order to understand if NFE could represent the basis to build a new biomaterial for oral soft tissue regeneration.

DATA AVAILABILITY STATEMENT

The data that support the findings of this study are available from the corresponding author upon reasonable request.

AUTHOR CONTRIBUTIONS

All the Authors contributed to conception and design of the study. EC and EA formulated and synthesized nanofibers. RD and AF characterized nanofibers. EC, FP, and DH performed morphological and *in vitro* study. NG and LD performed gene and protein expression analysis. NG and EC wrote the first

draft of the manuscript. DH and LD wrote sections of the manuscript. CD coordinated the project. All authors contributed to manuscript revision, read, and approved the submitted version.

ACKNOWLEDGMENTS

The Authors thank Dr. Kralovic Martin, Ing. Petr Novotný and Dr. Giuseppe Bitti, researchers at UCEEB, Czech Technical University, Trinecka 1024, 273 43 Bystřice nad Pernštejnem, Czech Republic, and Prof. Lina Altomare, Politecnico di Milano, for their precious contribution.

REFERENCES

- Ahadian, S., Finbloom, J. A., Mofidfar, M., Dilemiz, S. E., Nasrollahi, F., Davoodi, E., et al. (2020). Micro and Nanoscale Technologies in Oral Drug Delivery. *Adv. Drug Deliv. Rev.* 157, 37–62. doi:10.1016/j.addr.2020.07.012
- Alexander, S. A., and Donoff, R. B. (1980). The Glycosaminoglycans of Open Wounds. *J. Surg. Res.* 29, 422–429. doi:10.1016/0022-4804(80)90055-4
- Amler, E., Filová, E., Buzgo, M., Prosecká, E., Rampichová, M., Nečas, A., et al. (2014). Functionalized Nanofibers as Drug-Delivery Systems for Osteochondral Regeneration. *Nanomedicine* 9, 1083–1094. doi:10.2217/nnm.14.57
- Bertl, K., Bruckmann, C., Isberg, P.-E., Klinge, B., Gotfredsen, K., and Stavropoulos, A. (2015). Hyaluronan in Non-surgical and Surgical Periodontal Therapy: a Systematic Review. *J. Clin. Periodontol.* 42, 236–246. doi:10.1111/jcpe.12371
- Beznoska, J., Uhlík, J., Kestlerová, A., Královíč, M., Divín, R., Fedáčko, J., et al. (2019). PVA and PCL Nanofibers Are Suitable for Tissue Covering and Regeneration. *Physiol. Res.* 68, S501–S508. doi:10.33549/physiolres.934389
- Bhattarai, R., Bachu, R., Boddu, S., and Bhaduri, S. (2018). Biomedical Applications of Electrospun Nanofibers: Drug and Nanoparticle Delivery. *Pharmaceutics* 11, 5. doi:10.3390/pharmaceutics11010005
- Bonilla-Represa, V., Abalos-Labruzzi, C., Herrera-Martinez, M., and Guerrero-Pérez, M. O. (2020). Nanomaterials in Dentistry: State of the Art and Future Challenges. *Nanomaterials* 10, 1770. doi:10.3390/nano10091770
- Botelho, J., Cavacas, M. A., Machado, V., and Mendes, J. J. (2017). Dental Stem Cells: Recent Progresses in Tissue Engineering and Regenerative Medicine. *Ann. Med.* 49, 644–651. doi:10.1080/07853890.2017.1347705
- Brew, K., Dinakarpanian, D., and Nagase, H. (2001). Tissue Inhibitors of Metalloproteinases: Evolution, Structure and Function. *Biochim. Biophys. Acta* 1477, 267–283. doi:10.1016/s0167-4838(99)00279-4
- Burridge, K., and Gulluy, C. (2016). Focal Adhesions, Stress Fibers and Mechanical Tension. *Exp. Cel. Res.* 343, 14–20. doi:10.1016/j.yexcr.2015.10.029
- Campo, G. M., Avenoso, A., D'Ascola, A., Prestipino, V., Scuruchi, M., Nastasi, G., et al. (2012). Inhibition of Hyaluronan Synthesis Reduced Inflammatory Response in Mouse Synovial Fibroblasts Subjected to Collagen-Induced Arthritis. *Arch. Biochem. Biophys.* 518, 42–52. doi:10.1016/j.abb.2011.12.005
- Canciani, E., Dellavia, C., Ferreira, L. M., Giannasi, C., Carmagnola, D., Carrassi, A., et al. (2016). Human Adipose-Derived Stem Cells on Rapid Prototyped Three-Dimensional Hydroxyapatite/Beta-Tricalcium Phosphate Scaffold. *J. Craniofac. Surg.* 27, 727–732. doi:10.1097/SCS.00000000000002567
- Canciani, E., Sirello, R., Pellegrini, G., Henin, D., Perrotta, M., Toma, M., et al. (2021). Effects of Vitamin and Amino Acid-Enriched Hyaluronic Acid Gel on the Healing of Oral Mucosa: *In Vivo* and *In Vitro* Study. *Medicina* 57, 285. doi:10.3390/medicina57030285
- Carter, P., Rahman, S. M., and Bhattarai, N. (2016). Facile Fabrication of Aloe Vera Containing PCL Nanofibers for Barrier Membrane Application. *J. Biomater. Sci. Polym. Edition* 27, 692–708. doi:10.1080/09205063.2016.1152857
- Chanda, A., Adhikari, J., Ghosh, A., Chowdhury, S. R., Thomas, S., Datta, P., et al. (2018). Electrospun Chitosan/polycaprolactone-Hyaluronic Acid Bilayered Scaffold for Potential Wound Healing Applications. *Int. J. Biol. Macromolecules* 116, 774–785. doi:10.1016/j.ijbiomac.2018.05.099
- Chen, W. Y. J., and Abatangelo, G. (1999). Functions of Hyaluronan in Wound Repair. *Wound Repair Regen.* 7, 79–89. doi:10.1046/j.1524-475x.1999.00079.x
- Chopin-Doroteo, M., Salgado-Curiel, R. M., Pérez-González, J., Marín-Santibáñez, B. M., and Krötzsch, E. (2018). Fibroblast Populated Collagen Lattices Exhibit Opposite Biophysical Conditions by Fibrin or Hyaluronic Acid Supplementation. *J. Mech. Behav. Biomed. Mater.* 82, 310–319. doi:10.1016/j.jmbm.2018.03.042
- Dellavia, C., Ricci, G., Pettinari, L., Allievi, C., Grizzi, F., and Gagliano, N. (2014). Human Palatal and Tuberosity Mucosa as Donor Sites for ridge Augmentation. *Int. J. Periodontics Restorative Dent.* 34, 179–186. doi:10.11607/prd.1929
- Dupont, S., Morsut, L., Aragona, M., Enzo, E., Giulitti, S., Cordenonsi, M., et al. (2011). Role of YAP/TAZ in Mechanotransduction. *Nature* 474, 179–183. doi:10.1038/nature10137
- Eliezer, M., Sculean, A., Miron, R. J., Nemcovsky, C., Weinberg, E., Weinreb, M., et al. (2019). Hyaluronic Acid Slows Down Collagen Membrane Degradation in Uncontrolled Diabetic Rats. *J. Periodont Res.* 54, 644–652. doi:10.1111/jre.12665
- Francetti, L., Dellavia, C., Corbella, S., Cavalli, N., Moscheni, C., Canciani, E., et al. (2019). Morphological and Molecular Characterization of Human Gingival Tissue Overlying Multiple Oral Exostoses. *Case Rep. Dentistry* 2019, 1–10. doi:10.1155/2019/3231759
- Fraser, J. R. E., Laurent, T. C., and Laurent, U. B. G. (1997). Hyaluronan: its Nature, Distribution, Functions and Turnover. *J. Intern. Med.* 242, 27–33. doi:10.1046/j.1365-2796.1997.00170.x
- Gunn, J., and Zhang, M. (2010). Polyblend Nanofibers for Biomedical Applications: Perspectives and Challenges. *Trends Biotechnol.* 28, 189–197. doi:10.1016/j.tibtech.2009.12.006
- Hägi, T. T., Laugisch, O., Ivanovic, A., and Sculean, A. (2014). Regenerative Periodontal Therapy. *Quintessence Int.* 45, 185–192. doi:10.3290/j.qi.a31203
- Hatayama, T., Nakada, A., Nakamura, H., Mariko, W., Tsujimoto, G., and Nakamura, T. (2017). Regeneration of Gingival Tissue Using *In Situ* Tissue Engineering with Collagen Scaffold. *Oral Surg. Oral Med. Oral Pathol. Oral Radiol.* 124, 348–354. doi:10.1016/j.oooo.2017.05.471
- Hobson, R. (2016). Vitamin E and Wound Healing: an Evidence-Based Review. *Int. Wound J.* 13, 331–335. doi:10.1111/iwj.12295
- Jansen, K. A., Donato, D. M., Balcioglu, H. E., SchmidtDanen, T. E. H., Danen, E. H. J., and Koenderink, G. H. (2015). A Guide to Mechanobiology: where Biology and Physics Meet. *Biochim. Biophys. Acta (Bba) - Mol. Cel Res.* 1853, 3043–3052. doi:10.1016/j.bbamcr.2015.05.007
- Kalantary, S., Golbabaie, F., Latifi, M., Shokrgozar, M. A., and Yaseri, M. (2020). Feasibility of Using Vitamin E-Loaded Poly(ϵ -caprolactone)/Gelatin Nanofibrous Mat to Prevent Oxidative Stress in Skin. *J. Nanosci. Nanotechnol.* 20, 3554–3562. doi:10.1166/jnn.2020.17486
- Koniczka, P., Barszcz, M., Kowalczyk, P., Szlis, M., and Jankowski, J. (2019). The Potential of Acetylsalicylic Acid and Vitamin E in Modulating Inflammatory Cascades in Chickens under Lipopolysaccharide-Induced Inflammation. *Vet. Res.* 50, 65. doi:10.1186/s13567-019-0685-4
- Litwiniuk, M., Krejner, A., Speyrer, M. S., Gauto, A. R., and Grzela, T. (2016). Hyaluronic Acid in Inflammation and Tissue Regeneration. *Wounds* 28, 78–88. doi:10.37473/dac/10.1101/2020.06.02.20120733

- Mesa, F. L., Aneiros, J., Cabrera, A., Bravo, M., Caballero, T., Revelles, F., et al. (2002). Antiproliferative Effect of Topic Hyaluronic Acid Gel. Study in Gingival Biopsies of Patients with Periodontal Disease. *Histol. Histopathol.* 17, 747–753. doi:10.14670/HH-17.747
- Mohandesnezhad, S., Pilehvar-Soltanahmadi, Y., Alizadeh, E., Goodarzi, A., Davaran, S., Khatamian, M., et al. (2020). *In Vitro* evaluation of Zeolite-nHA Blended PCL/PLA Nanofibers for Dental Tissue Engineering. *Mater. Chem. Phys.* 252, 123152. doi:10.1016/j.matchemphys.2020.123152
- Murphy, G., Willenbrock, F., Crabbe, T., O'Shea, M., Ward, R., Atkinson, S., et al. (1994). Regulation of Matrix Metalloproteinase Activity. *Ann. NY Acad. Sci.* 732, 31–41. doi:10.1111/j.1749-6632.1994.tb24722.x
- Pirnazar, P., Wolinsky, L., Nachnani, S., Haake, S., Piloni, A., and Bernard, G. W. (1999). Bacteriostatic Effects of Hyaluronic Acid. *J. Periodontol.* 70, 370–374. doi:10.1902/jop.1999.70.4.370
- Plencner, M., East, B., Litvinec, A., Buzgo, M., Tonar, Z., Otahal, M., et al. (2014). Abdominal Closure Reinforcement by Using Polypropylene Mesh Functionalized with Poly- ϵ -Caprolactone Nanofibers and Growth Factors for Prevention of Incisional Hernia Formation. *Ijn* 9, 3263–3277. doi:10.2147/IJN.S63095
- Price, R. D., Myers, S., Leigh, I. M., and Navsaria, H. A. (2005). The Role of Hyaluronic Acid in Wound Healing. *Am. J. Clin. Dermatol.* 6, 393–402. doi:10.2165/00128071-200506060-00006
- Primpke, S., Wirth, M., Lorenz, C., and Gerdts, G. (2018). Reference Database Design for the Automated Analysis of Microplastic Samples Based on Fourier Transform Infrared (FTIR) Spectroscopy. *Anal. Bioanal. Chem.* 410, 5131–5141. doi:10.1007/s00216-018-1156-x
- Rasperini, G., Pilipchuk, S. P., Flanagan, C. L., Park, C. H., Pagni, G., Hollister, S. J., et al. (2015). 3D-printed Bioresorbable Scaffold for Periodontal Repair. *J. Dent. Res.* 94, 153S–157S. doi:10.1177/0022034515588303
- Rasperini, G., Tavelli, L., Barootchi, S., McGuire, M. K., Zucchelli, G., Pagni, G., et al. (2020). Interproximal Attachment Gain: The challenge of Periodontal Regeneration. *J. Periodontol.* 2020, 1–16. doi:10.1002/JPER.20-0587
- Robert, L. (2015). Hyaluronan, a Truly “Youthful” Polysaccharide. Its Medical Applications. *Pathologie Biologie* 63, 32–34. doi:10.1016/j.patbio.2014.05.019
- Sakai, T., and Gross, J. (1967). Some Properties of the Products of Reaction of Tadpole Collagenase with Collagen*. *Biochemistry* 6, 518–528. doi:10.1021/bi00854a021
- Seo, S.-J., Kim, H.-W., and Lee, J.-H. (2016). Electrospun Nanofibers Applications in Dentistry. *J. Nanomater.*, 2016, 1, 7. doi:10.1155/2016/5931946
- Silver, F. H., Christiansen, D., Snowhill, P. B., Chen, Y., and Landis, W. J. (2000). The Role of mineral in the Storage of Elastic Energy in turkey Tendons. *Biomacromolecules* 1, 180–185. doi:10.1021/bm9900139
- Tammi, M. I., Day, A. J., and Turley, E. A. (2002). Hyaluronan and Homeostasis: a Balancing Act. *J. Biol. Chem.* 277, 4581–4584. doi:10.1074/jbc.R100037200
- Thiele, J. J., Hsieh, S. N., and Ekanayake-Mudiyansele, S. (2005). Vitamin E: Critical Review of its Current Use in Cosmetic and Clinical Dermatology. *Dermatol. Surg.* 31, 805–813. doi:10.1111/j.1524-4725.2005.31724
- Totaro, A., Panciera, T., and Piccolo, S. (2018). YAP/TAZ Upstream Signals and Downstream Responses. *Nat. Cel Biol.* 20, 888–899. doi:10.1038/s41556-018-0142-z
- Voigt, J., and Driver, V. R. (2012). Hyaluronic Acid Derivatives and Their Healing Effect on burns, Epithelial Surgical Wounds, and Chronic Wounds: A Systematic Review and Meta-Analysis of Randomized Controlled Trials. *Wound Repair Regen.* 20, 317–331. doi:10.1111/j.1524-475X.2012.00777.x
- Walker, L., Overstreet, M., and Yeowell, H. (2005). Tissue-specific Expression and Regulation of the Alternatively-Spliced Forms of Lysyl Hydroxylase 2 (LH2) in Human Kidney Cells and Skin Fibroblasts. *Matrix Biol.* 23, 515–523. doi:10.1016/j.matbio.2004.11.002
- Wang, J. H.-C., Guo, Q., and Li, B. (2012). Tendon Biomechanics and Mechanobiology-A Minireview of Basic Concepts and Recent Advancements. *J. Hand Ther.* 25, 133–141. doi:10.1016/j.jht.2011.07.004
- Wang, M., Roy, A. K., and Webster, T. J. (2017). Development of Chitosan/Poly(Vinyl Alcohol) Electrospun Nanofibers for Infection Related Wound Healing. *Front. Physiol.* 7, 683. doi:10.3389/fphys.2016.00683
- Woessner, J. F. (1991). Matrix Metalloproteinases and Their Inhibitors in Connective Tissue Remodeling. *FASEB j.* 5, 2145–2154. doi:10.1096/fasebj.5.8.1850705

Conflict of Interest: The authors declare that the research was conducted in the absence of any commercial or financial relationships that could be considered as a potential conflict of interest.

Copyright © 2021 Canciani, Gagliano, Paino, Amler, Divin, Denti, Henin, Fiorati and Dellavia. This is an open-access article distributed under the terms of the Creative Commons Attribution License (CC BY). The use, distribution or reproduction in other forums is permitted, provided the original author(s) and the copyright owner(s) are credited and that the original publication in this journal is cited, in accordance with accepted academic practice. No use, distribution or reproduction is permitted which does not comply with these terms.